CHEMICAL ENGINEERING TRANSACTIONS
VOL. 53, 2016
A publication of AIDIC
The Italian Association of Chemical Engineering
Online at www.aidic.it/cet
Guest Editors: Valerio Cozzani, Eddy De Rademaeker, Davide Manca

ISBN 978-88-95608-44-0; **ISSN** 2283-9216
DOI: 10.3303/CET1653059

Numerical Modeling of Experimental Trials Involving Pressurized Release of Gaseous CO_2

Paolo Mocellin, Giuseppe Maschio*

University of Padova, Department of Industrial Engineering, Via Marzolo 9, 35131 Padova, Italy.
giuseppe.maschio@unipd.it

Modeling pressurized releases in QRA procedures is a key step in obtaining a reliable description and prediction of hazards. The application of these procedures to hazards related to CCS and EOR infrastructures poses many problems strictly related to the peculiar thermodynamic behaviour of the CO_2 (Koorneef et al, 2009). Difficulties in the prediction of the discharge behaviour of the CO_2 during rapid depressurizations can influence calculations concerning the atmospheric dispersion and the eventuality of a dry ice bank formation (Mocellin et al., 2015).
In order to fill some gaps concerning especially compressible CO_2 discharges, starting from self – collected laboratory scale experimental data, a semi – predictive model is proposed with the aim of describing a sudden release from a pressurized vessel.
The model is based both on conservation equations as well as suitable correlations to give a description of heat – transfer mechanisms. In addition, the Peng – Robinson equation of state is employed in order to predict the CO_2 thermodynamic behaviour and to correctly manage both the gaseous and the dense phase if necessary.
The application of the model shows good agreement with the experimental data series, especially in terms of pressure profiles and discharge time. In addition, the vessel thermal dynamics is adequately predicted both for the releases at higher pressure investigated especially when related to an internal surface temperature experimentally derived.

1. Introduction

Unlike consequences estimation procedures applied to Gas&Oil process industries, the description of hazards related to the handling of CO_2 must deal with the lack of experimental data, historical statistics and the complex thermodynamic behavior of this substance (Mahgerefteh et al., 2016).
The deployment of CO_2 infrastructures for CCS (Carbon Capture and Storage) and EOR (Enhanced Oil Recovery) targets will take place in coming decades complaining the needs to control the so called Global Warming. However, the deficiency in the number of installed plants makes it difficult to schedule a comprehensive hazards analysis because of the lack in the knowledge of main phenomena related to a rapid CO_2 depressurization. A huge scientific effort is now oriented towards both the experimental and the theoretical investigation of these releases in order to make available models to be reliably applied to the case of the CO_2 (Witlox et al., 2014).
It should be noted that actually the quantitative estimation of the release scenarios involving CO_2 is affected by many uncertainties concerning primarily:

- the thermodynamic models to be employed in the description of CO_2 properties;
- the prediction of dense phase appearance (liquid and solid) during the expansion;
- the applicability of VBM (Vessel Blowdown models) to general CO_2 releases.

All of these aspects should be at least considered during the modeling of releases involving CO_2 because its peculiar behavior when subjected to high pressure gradients that may lead to liquid and solid phase appearance.
However, the lack of experimental data does actually allow for only limited validation procedures.

Please cite this article as: Mocellin P., Maschio G., 2016, Numerical modeling of experimental trials involving pressurized release of gaseous co2, Chemical Engineering Transactions, 53, 349-354 DOI: 10.3303/CET1653059

Therefore, starting from self – made laboratory scale experimental data, a model is proposed with the aim to give reasons to collected observations. Experimental data (Mocellin et al., 2016) concern gaseous CO_2 expansions from a filling tank maintained at controlled conditions. Stagnation conditions refers to pressures up to 45 barg and temperatures in the range 0 – 40 °C and varying them, pressure and temperature profiles are collected during the rapid depressurizations. Both internal and external wall temperatures are recorded in order to have information on temperature gradients governing also heat – transfer mechanism between the flowing CO_2 and the stainless steel walls.

2. Constitutive Equations and Thermodynamic Model

The discharge from a pressurized vessel through an orifice is a transient phenomenon characterized by the appearance of pressure and temperature gradients. The pressure difference is the main release governing force with the presence of the solid stainless steel walls acting as the principal source of heat – exchange driven mechanisms.
The transient model consists of the conservation equations as well as all relationships concerning heat – transfer mechanisms and friction losses during the compressible CO_2 flow across the system.
A schematic representation of the system under investigation is reported in Figure 1.

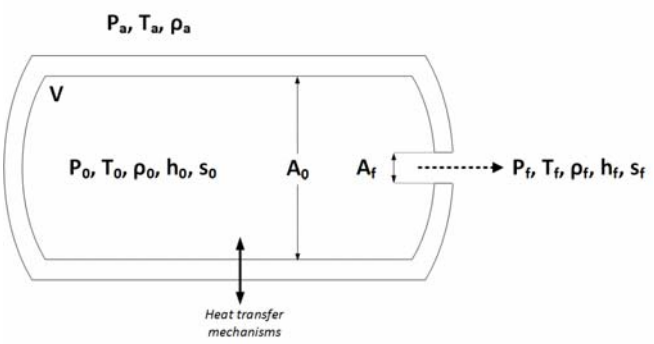

Figure 1: schematic representation of the discharge vessel with an indication of the pertinent properties required.

Considering Figure 1, applicable transient conservation equations are the mass and the energy balance as respectively reported in Eq. (1) – (2):

$$\frac{d}{dt}(\rho_0 V) = V\frac{d\rho_0}{dt} = -\dot{m}_0 \tag{1}$$

$$V\left[\rho_0\frac{d\widetilde{u_0}}{dt} + \widetilde{u_0}\frac{d\rho_0}{dt}\right] = -\dot{m}_0\left(\widetilde{u_0} + \frac{P_0}{\rho_0}\right) + \dot{q}_v A_{int,v} \tag{2}$$

In Eq. (1) – (2), ρ_0 is the instantaneous CO_2 density inside the vessel, V the vessel volume, $\dot{m}_0$ the mass flux of CO_2 leaving the system, $\widetilde{u_0}$ the specific CO_2 internal energy, P_0 the CO_2 pressure inside the vessel, $\dot{q}_v$ the heat flux at the vessel wall and $A_{int,v}$ the internal vessel surface area.
The closure of the model requires the estimation of $\dot{m}_0$ that is based on the application of mass, mechanical energy conservation and momentum balances in the path towards the orifice leading to Eq. (3):

$$\dot{m}_0 = \gamma_d \rho_1 A_f \sqrt{\left[-2\left(\int_0^1 \rho^{-1} dP + \frac{1}{2}\langle v_1\rangle^2 \sum_i \varphi_i\right)\right]\left[1 - \left(\frac{\rho_1 A_f}{\rho_0 A_0}\right)^2\right]} \tag{3}$$

Eq. (3) gives $\dot{m}_0$ as a function of instantaneous thermodynamic properties variation between the stagnation conditions and those at the discharging orifice. The integral comparing in Eq. (3) accounts for the thermodynamic pathway followed by the CO_2 during the expansions thus requiring an EoS model and a $T = T(P)$ mathematical relation. This relation can be assumed (e.g. isentropic, isenthalpic, isothermal, …) or can be derived from the experimentally measured couples (P, T) as in the present case.
The term containing the friction loss factors φ_i accounts for pressure drops induced by obstacles during the CO_2 flow that are mainly represented by the sudden constriction and the discharging orifice.

The analysis of the heat – transfer phenomena is performed by means of suitable correlations describing the main mechanisms that are taking place during the depressurization. Among these both the natural and forced convection inside the tank as well as the conduction across the stainless steel wall and the insulation are modeled.
Required CO_2 properties are derived from the cubic Peng – Robinson equation of state which is considered to be robust enough and easy to implement.

3. Results and Discussion

Model performances are assessed in terms of pressure and temperature profiles prediction with respect to the time. Therefore, starting from the initial conditions expressed in terms of $P_0(t=0)$ and $T_0(t=0)$ imposed during the experimental trials, the model is run against the available profiles in order to verify its reliability.
Eq. (1) – (3) are numerically managed by means of an implicit Runge – Kutta scheme based on Gauss methods.

3.1 Pressure profiles

The results analysis firstly focuses on the depressurization profiles expressed in terms of vessel pressure variations with respect to time.
The dynamics of the vessel pressure, assumed to be uniformly distributed inside the storage tank, is the result of both the gradients existing between the stagnation conditions and the atmospheric environment as well as the pressure drops induced by the flow across the constriction and the orifice.
Considering the CO_2 expansions from 15 and 35 barg and 25 °C, Figure 2 a comparison between the internal vessel pressure experimental profile and that predicted by the model.

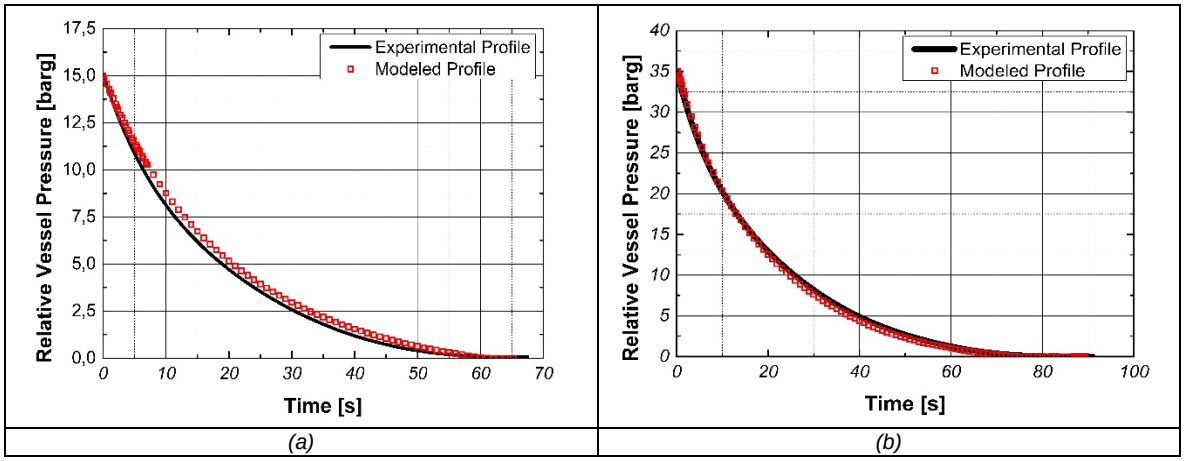

Figure 2. Comparison between the experimental internal vessel pressure profile and that predicted by the model. a- depressurization from 15 barg and 25 °C; b- depressurization from 35 barg and 25 °C.

The predicted pressure trends, as emerged by the application of the model presented in section 2, are in good agreement with the experimental data profiles and are caught especially in the initial stages. Some deviations from the real behavior are observed in the intermediate stages where temperature gradients are more significant.
Simulation runs show that the best agreement with the experimentally observed behavior is obtained with increasing initial stagnation pressures and temperatures. However, the combination of the proposed model with the assumption of ideal gas behavior fails to predict the pressure trends for charging pressures higher than 20 barg. This proving the relevance of the specific thermodynamic model employed in the description of both the CO_2 properties and the expansion pathway that should include the non – ideal characterization.
It should be noted that in modeling the depressurization profile, a value for γ_d in Eq. (3) must be allocated, that is a value for the discharge coefficient across the orifice needs to be assumed or experimentally obtained. In this case, starting from the experimental data, each experimental trial has been characterized with a time – dependent γ_d based on the pressure drops measure across the orifice. Results obtained in Figure 2 however pertain to a time – integral weighted average in order to replace the γ_d time profile with a single averaged value.
Table 1 collects the values of γ_d resulting from the averaging procedure of the experimental data profiles.

In addition, the predicted discharge time shows good agreement with the experimental data (Mocellin et al., 2016) being this parameter strictly related to the pressure profile and slightly variable with the initial charging temperature.

Table 1: Averaged γ_d to be used in Eq. (3) with respect to experimental initial conditions.

Pressure [barg]	Temperature [°C]	γ_d [-]	Pressure [barg]	Temperature [°C]	γ_d [-]
10	20	0,210	20	20	0,184
10	30	0,227	20	30	0,188
15	20	0,192	35	20	0,169
15	30	0,198	35	30	0,174

3.2 Temperature profiles

The experimental time temperature profiles, concerning a single – phase release, display a characteristic trend concerning an initial decreasing behavior finally rising to the equilibrium environmental conditions. The early drop is mainly induced by the pressure variations occurring inside the tank while the subsequent temperature rise is governed by the heat transfer mechanisms that are taking place between the decreasing CO_2 mass and the vessel walls.
Figure 3 gives a representation of the modeled inside vessel temperature with respect to the experimental measures.

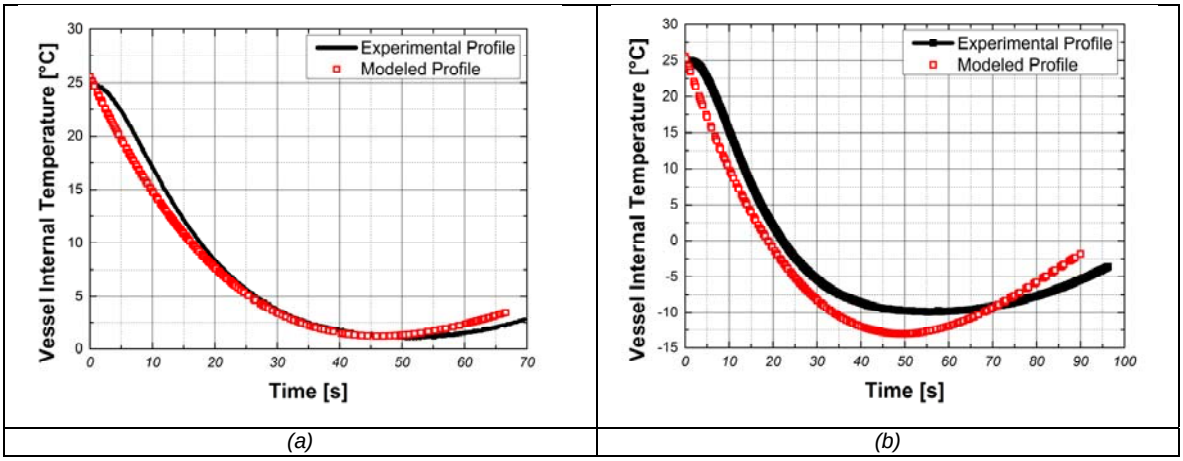

Figure 3. Comparison between the experimental internal vessel temperature profile and that predicted by the model. a- depressurization from 15 barg and 25 °C; b- depressurization from 35 barg and 25 °C.

Considering Figure 3, the match between the predicted and the measured temperature profile is depending on the operative conditions. Temperature dynamics linked to lower operative pressures are better predicted than those concerning higher initial charging pressures.
The matching of the temperature profile should involve both the dynamics and the minimum reached temperature. The latter is the result of the balance between the mechanical contribution induced by the pressure gradients and the flux of heat from the vessel walls.
It should be noted that in the case of the 15 barg depressurization, both are well predicted indicating that the pressure dynamics and the modeled heat transfer between the discharging CO_2 and the walls are substantially well chosen. However, increasing the initial charging pressure, the model lacks the experimental profiles especially in the region concerning heat transfer induced mechanisms with the walls.
Differences between the profiles are observed for charging pressure higher than 28 barg.
Considering Figure 3-b, while the initial decreasing contribution in the temperature is caught by the model even if leading to a minimum temperature lower than that measured, the final trend does not respond to the real behavior. In general, the heating mechanisms lead to a higher temperature than those observed and the gap between the profiles grows with increasing initial charging pressures.
The main reason is related to the descriptive models of the heat transfer mechanisms and issues concerning the choice of the wall temperatures.

In this sense, considered that heat transfer mechanisms are various (internal convection, conduction and external convection), during the depressurizations they assume different importance depending on the relative governing driving force. First steps are mainly governed by the pressure gradients and the thermodynamic transformation that is taking place while once the pressure differences are small, the presence of the warmer wall acts as a source of heat. The transfer from this source is modeled by means of the description of both the conductive and the convective contributions with an internal superficial temperature assumed to be equal to the mean value between the bulk temperatures. This assumption deals with the lack of the experimental datum concerning the internal surface temperature that is not collectable. Therefore, inaccuracies in the modeling procedure may arise especially when the hypothesis appears to be restrictive that is for trials involving larger temperature gradients (i.e. expansions from the highest initial charging pressures).
It should be noted that a temperature difference between the internal CO_2 domain and the external wall vessel always exists during the depressurization making rise to a heat transfer toward the internal domain as indicated in Figure 4 referred to the 35 barg expansion.

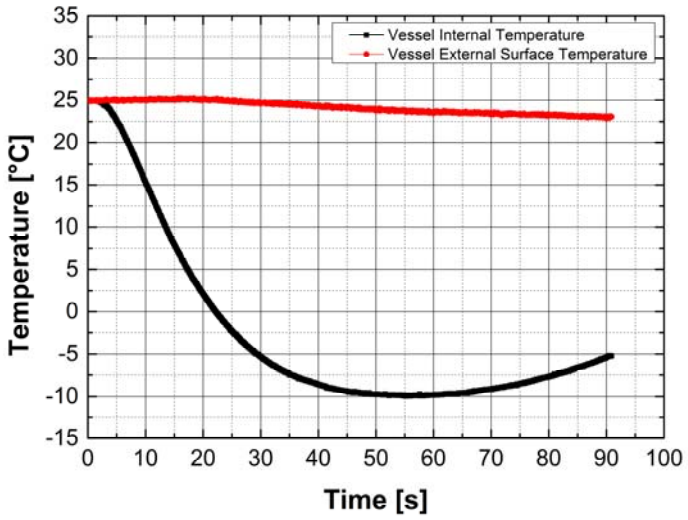

Figure 4. 35 barg depressurization. Experimental measured internal and external surface vessel temperature.

The inclusion in the model of an internal surface temperature averaged from the experimental data gives rise to a better match of the modeled profiles also for the expansions at higher pressures with predicted values fully corresponding to measured data.
In addition, the simulation runs allow for the determination of a global heat transfer coefficient that can be defined with respect to both the internal CO_2 domain and the external vessel surface. While the external heat transfer coefficient usually takes orders of magnitude of 10 – 20 $kJh^{-1}m^{-2}°C^{-1}$, the internal heat transfer coefficients show a marked variability depending on the initial charging pressure with peak values obtained at the lowest temperatures and of the order of 55 and 180 $kJh^{-1}m^{-2}°C^{-1}$ respectively for the expansions starting from 15 and 35 barg.

3.3 Expansion efficiency

A measure of the modeled expansion efficiency can be assessed to give a reasonable idea of the nature of the expansion that is taking place because of the pressure gradients.
In the present investigation the efficiency gives a measure of the deviation of the process from a depressurization that is taking place without any occurring heat exchange phenomenon in terms of the work done on the surroundings by the expanding CO_2.
The two theoretical limits can be identified as an isentropic expansion, leading to the lowest temperature, and an isenthalpic depressurization, leading to less drastic temperature drop.
Considering different simulation trials with respect to the experimental data, Table 2 gives an indication of the efficiency expressed as percentage with respect to the full isentropic expansion (100 %) and completely isenthalpic depressurization (0 %).
As indicated all the reported tests are characterized by an intermediate behavior in the sense that heat exchanges are allowed even if the expansions are extremely rapid. Neither the conservation of the entropy nor

that of the enthalpy can be assumed. With increasing charging pressures, the expansion moves toward higher efficiencies but all trials show that its value is limited to 70 % for the 45 barg depressurizations.

Table 2: Expansion efficiencies with respect to theoretical depressurizations.

Initial Pressure [barg]	Initial Temperature [°C]	Efficiency [%]
10	20	42
10	30	46
15	20	45
15	30	42
20	20	48
20	30	46
35	20	61
35	30	56

4. Conclusions

A transient model descriptive of a rapid vessel depressurization filled with gaseous CO_2 is proposed. The model, relying on conservation equations and a suitable EoS, has the aim of giving a description of both the temperature and the pressure profiles arising from the expansion.

Considering the available experimental data, the suggested model is capable to fit considerably all the experimental pressure profiles up to 45 barg charging pressures. Also the discharge time is well predicted being strictly linked to the pressure dynamics.

Temperature profiles, involving gradients induced by heat transfer mechanisms with the vessel walls and pressure variations, are partially matched especially with reference to the heating step induced by the warmer wall. The use of an internal surface vessel temperature obtained from the experimental data increases the model capability to predict the characteristic temperature profile.

Calculated internal global heat transfer coefficient shows a relevant heat exchange with the vessel walls quantified in values higher than 50 $kJh^{-1}m^{-2}°C^{-1}$.

A comparison of the mechanical work induced by the expanding CO_2 with reference to that pertaining to the theoretical depressurization profiles allows to state that all pathways are intermediate between a constant enthalpy and entropy transformation. While a variation in the charging temperature does not induced noticeable variations, an increase in the storage pressure tends to move the transformation towards an enhanced isentropic indicator.

References

Kornneef, J., Spruijt, M., Molag, M., Ramirez, A., Faaij, A., Turkenburg, W., 2009. Uncertainties in Risk Assessment of CO_2 Pipelines. Energy Procedia, 1(1), 1587 – 1594.

Mahgerefteh, H., Sundara, V., Brown, S., Martynov, S., 2016. Modelling Emergency Isolation of Carbon Dioxide Pipelines. International Journal of Greenhouse Gas Control, 44, 88 – 93.

Mocellin P., Vianello, C., Maschio, G., 2015. Carbon Capture and Storage Hazard Investigation: Numerical Analysis of Hazards Related To Dry Ice Bank Sublimation Following Accidental Carbon Dioxide Releases. Chemical Engineering Transactions, 43, 1897 – 1902.

Mocellin, P., Vianello, C., Maschio, G., 2016. CO_2 Transportation Hazards in CCS and EOR Operations: Preliminary Lab – scale Experimental Investigation of CO_2 Pressurized Releases. Chemical Engineering Transactions, 48 (under publication).

Witlox, H.W.W., Stene, A., Harper, M., Oke, A., Stene, J., 2014. Validation of Discharge and Atmospheric Dispersion for Unpressurized and Pressurized Carbon Dioxide Releases. Process Safety and Environmental Protection, 92, 3 – 16.